Hindawi
Mathematical Problems in Engineering
Volume 2020, Article ID 7204859, 8 pages
https://doi.org/10.1155/2020/7204859

Research Article

Analysis of Leakage Model of All-Metal Screw Pump

Heng Zhang, Xiaodong Wu, and Yongsheng An

MOE Key Laboratory of Petroleum Engineering, China University of Petroleum-Beijing, Beijing 102249, China

Correspondence should be addressed to Heng Zhang; zhangheng4212@163.com

Received 16 March 2020; Accepted 15 May 2020; Published 27 May 2020

Academic Editor: Francesco Pellicano

Traditional rubber screw pumps use an interference method to engage. When the pressure is less than the breakdown pressure of the pump, there is no leakage in the pump. The all-metal screw pump stator and rotor are made of metal, and the stator and rotor adopt a gap-fitting engagement method, so even when the pump is working normally, the leakage is objective. Based on the concentric annular gap flow, the pressure drop leakage caused by the fluid inertia force is fully considered, and the calculation formula of the leakage of the all-metal screw pump is studied from the three aspects of transverse leakage, longitudinal leakage, and oblique leakage. This model was experimentally verified by a commercial all-metal screw pump produced by Shihong Petroleum Equipment Company. The model results show that the leakage of the all-metal screw pump is mainly affected by the structure parameters of the pump itself and the density of the pumped fluid, and the gap height is the main factor affecting the leakage.

1. Introduction

As a new mechanical oil extraction equipment, the screw pump has many advantages, such as simple structure and stable displacement [1, 2]. The stator and rotor of traditional screw pumps are made of rubber, which is inexpensive, but the pressure at the exit of the pump is large, and it is easy to be broken down [3]. It is not suitable for high temperature and high pressure working environments, so its application has certain limitations [4–7]. The stator and rotor of the all-metal screw pump are made of metal materials and are regarded as a new generation of screw pumps [8–10], especially in the fields of heavy oil thermal recovery, which are widely used [11, 12].

Due to the gap between the stator and the rotor of the all-metal screw pump, it is very necessary to study the leakage of the pump. The researchers used digital simulation software (CFD) to study the relevant leakage laws [13–18], but the digital analog analysis often ignored the complicated working conditions at the site which would cause a large error between the analysis results and the actual situation. The combination of theoretical modeling and experimental methods can avoid the above situation. Through theoretical modeling and experimental methods, Gamboa et al. [19, 20] determined that the pressure in the cavity of the all-metal screw pump is linearly distributed. Pessoa et al. [21] analyzed the leakage in the pump by establishing a flow model. Nguyen et al. [22], on the basis of the leakage in the pump, established a new fluid model to simulate the actual flow of the fluid, but they all only considered the influence of the viscous force and did not consider the effect of the inertial force of the fluid.

In view of this, there is currently a lack of a full metal screw pump leakage calculation model that fully considers the inertia of the fluid. The purpose of this article is to establish a new model of the full metal screw pump leakage. Compared with the existing models, the new model not only fully considers the inertial force of the fluid but also conducts research in three aspects: transverse leakage, longitudinal leakage, and oblique leakage. The model can also provide guidance for the design and optimization of field pumps.

2. Study on Leakage Mechanism

2.1. Model Simplification. Based on the structural characteristics and working principle of the clearance fit of the stator and rotor of the all-metal screw pump, the model makes the following assumptions:

(1) The fluid in the pump is pure liquid phase with constant temperature

(2) The fluid in the pump is Newtonian fluid, and the fluid meets Newton's internal friction law

(3) Uniform pressure changes between pumps

(4) The fluid properties are stable and do not change with pressure

Using the concentric ring gap flow theory [23], the pressure drop formula can be obtained as

$$\Delta p_0 = \frac{16\mu L}{\pi(R_0 + r_0)h^3} q, \tag{1}$$

where Δp_0 is the single-stage pressure difference between the pumps, Pa; μ is the viscosity of the fluid, Pa·s; L is the gap length, m; q is the gap leakage, m^3/s; r_0 and R_0 are the inner and outer radius of the concentric ring, m; and h is the height of the gap, m.

Now consider the pressure drop loss caused by the fluid inertia force.

2.1.1. Inlet Inertia Effect. As shown in Figure 1, the inner diameter of the ring is r_0, the outer diameter is R_0, and the fluid density is ρ, and it flows in at the velocity of u_0 from the inlet. After time dt, the velocity becomes u. In this process, the expression of fluid kinetic energy can be obtained as

$$\mathrm{d}E = \frac{\rho}{2}\pi\left(R_0^2 - r_0^2\right)d_r d_l\left(u^2 - u_0^2\right). \tag{2}$$

Assuming the initial velocity of the fluid is 0, equation (2) can be simplified as

$$\mathrm{d}E = \frac{\rho}{2}\pi\left(R_0^2 - r_0^2\right)d_r d_l u^2. \tag{3}$$

Further, the change in power can be expressed as

$$\mathrm{d}N = \frac{\mathrm{d}E}{\mathrm{d}t} = \frac{\rho}{2}\pi\left(R_0^2 - r_0^2\right)d_r u^3. \tag{4}$$

By integrating equation (4), the inertial power at the entrance can be obtained as

$$N = \frac{\rho}{2}\pi\left(R_0^2 - r_0^2\right)\int_{r_0}^{R_0} u^3 d_r. \tag{5}$$

Introduce the *N-S* equation in the cylindrical coordinate system because $f_x = f_y = f_z = 0$ and set the liquid flow condition to one-dimensional flow and axisymmetric, and we can get

$$\frac{\mathrm{d}^2 u}{\mathrm{d}r^2} + \frac{1}{r}\frac{\mathrm{d}u}{\mathrm{d}r} - \frac{1}{\mu}\frac{\mathrm{d}p}{\mathrm{d}x} = 0. \tag{6}$$

And the following relationship exists:

$$\frac{\mathrm{d}p}{\mathrm{d}x} = -\frac{\Delta p}{L}. \tag{7}$$

Taking equation (7) into equation (6) and integrating it, we can get

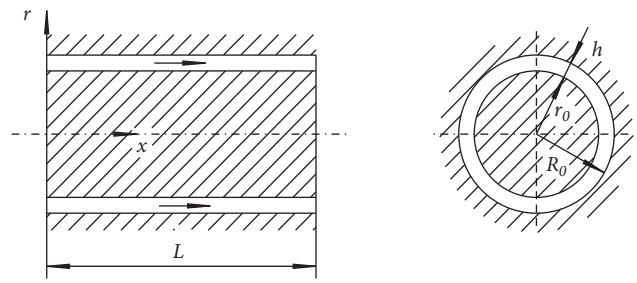

Figure 1: Concentric ring gap flow model.

$$u = C_1 \ln r - \frac{\Delta p}{4\mu L} r^2 + C_2, \tag{8}$$

where C_1 and C_2 are integral constants.

The boundary condition relation is

$$\begin{cases} u = 0; \ (r = r_0), \\ u = 0; \ (r = R_0). \end{cases} \tag{9}$$

Substituting formula (9) into formula (8), we can get

$$u = \frac{\Delta p}{4\mu L}\left(\frac{R_0^2 \ln(r/r_0) - r_0^2 \ln(r/R_0)}{\ln(R/r_0)} - r^2\right). \tag{10}$$

Substituting formula (10) into formula (5), we can get

$$N = \frac{48}{35}\frac{\rho q^3}{\pi^2 \overline{d}^2 h^2}, \tag{11}$$

where N is the inertial power at entrance, W; ρ is fluid density, kg/m^3; and $\overline{d}$ is the average diameter of the gap, m.

And there is a relation:

$$\begin{cases} h = R_0 - r_0, \\ \overline{d} = R_0 + r_0. \end{cases} \tag{12}$$

From equation (11), we can get the inertia pressure loss at the inlet section:

$$\Delta p_1 = \frac{N}{q} = \frac{48}{35}\frac{\rho q^2}{\pi^2 \overline{d}^2 h^2}, \tag{13}$$

where Δp_1 is the inertia pressure loss at the inlet section, Pa.

2.1.2. Exit Inertia Effect. For the exit inertia effect of the annular gap flow model, the pressure drop can be calculated by the following formula:

$$\Delta p_2 = \xi\frac{\rho}{2}\left(\frac{q}{\pi \overline{d} h}\right)^2, \tag{14}$$

where Δp_2 is the inertia pressure loss at the outlet section, Pa, and ξ is the sudden expansion pressure loss coefficient of the annular gap flow channel, and the value is 1.

The total pressure drop of the fluid through the model is obtained:

$$\Delta p = \Delta p_0 + \Delta p_1 + \Delta p_2 = \frac{16\mu L}{\pi \overline{d} h^3} q + \frac{131}{70}\rho\left(\frac{q}{\pi \overline{d} h}\right)^2. \quad (15)$$

Simplify equation (15) and solve the one-variable quadratic equation:

$$q = \frac{\pi \overline{d}}{h}\left(\sqrt{\frac{313600\mu^2 L^2}{17161\rho^2} + \frac{70h^4\Delta p}{131\rho}} - \frac{560\mu L}{131\rho}\right). \quad (16)$$

Equation (16) is the formula for calculating total leakage in the case of clearance fit of the all-metal screw pump. Analyze the effect of gap length on the amount of leakage. When $L = 0$, equation (16) can be simplified as

$$q = \frac{\pi \overline{d}}{h}\sqrt{\frac{70h^4\Delta p}{131\rho}} = \pi \overline{d} h\sqrt{\frac{70\Delta p}{131\rho}}. \quad (17)$$

Equation (17) considers only the leakage under the influence of inertial force, and the amount of leakage is proportional to the gap height and inversely proportional to the square root of the fluid density.

When L approaches positive infinity, formula (15) is simplified as

$$\Delta p = \frac{16\mu L}{\pi \overline{d} h^3} q\left(1 + \frac{131\rho q h}{1120\pi \overline{d}\mu L}\right). \quad (18)$$

It is further simplified to

$$q = \frac{\pi \overline{d} h^3}{16\mu L\left(1 + \left(131\rho q h/1120\pi \overline{d}\mu L\right)\right)}\Delta p. \quad (19)$$

Because $L \longrightarrow \infty$,

$$1 + \frac{131\rho q h}{1120\pi \overline{d}\mu L} \approx 1. \quad (20)$$

Therefore, equation (19) becomes

$$q = \frac{\pi \overline{d} h^3}{16\mu L}\Delta p. \quad (21)$$

It can be seen that formula (21) is the same as formula (1), which shows that if the inertial force of the fluid is not considered, the leakage of the all-metal screw pump is inversely proportional to the pressure difference and decreases with the increase of the viscosity of the lifting fluid.

2.2. Mathematical Modeling

2.2.1. Analysis of Leakage Process. According to the special meshing method and movement mechanism between the stator and rotor of the all-metal screw pump, the leakage process mainly includes horizontal and vertical leakage, as well as a small amount of oblique leakage, as shown in Figure 2, where the red a-cavity, c-cavity, and e-cavity are relatively high-pressure cavities, while the green b-cavity, d-cavity, and f-cavity are relatively low-pressure cavities.

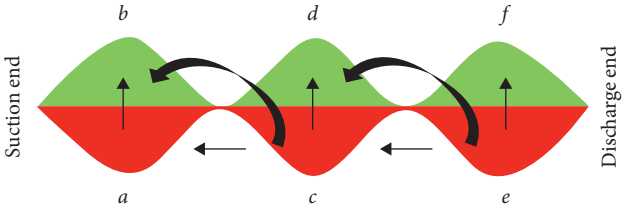

Figure 2: Leakage diagram of pump.

In summary, the leakage process mainly includes the following three types:

(1) Transverse leakage: as shown in the green and red parts in Figure 2, the corresponding liquid will leak into the relatively low-pressure cavity along the relatively high-pressure cavity, that is, from a to b, c to d, and e to f.

(2) Longitudinal leakage: after different low-pressure and high-pressure zones are formed in the radial direction, the corresponding low-pressure and high-pressure zones continue to increase in pressure from the suction end to the discharge end in the axial direction. That is to say, the pressures in the b, d, and f chambers are constantly increasing, and the pressures in the a, c, and e chambers are also increasing, so there is a leakage in the longitudinal direction from the high pressure region to the low pressure region, that is, f to d and d to b and e to c and c to a.

(3) Oblique leakage: when the fluid in the upper-stage high-pressure chamber flows in the axial direction to the lower-stage chamber, most of the fluid flows to the relatively high-pressure area on the same side, but a small amount of fluid flows into the relatively low-pressure chamber, so oblique leakage occurs, that is, fluid leakage occurs between the high-pressure chambers and low-pressure chambers in the axial direction. Because the oblique leakage fluid must not only overcome the pressure loss in the longitudinal direction but also overcome the pressure loss in the transverse direction, compared to the transverse and longitudinal leakage, the amount of oblique leakage is small, which is the secondary leakage of the entire pump.

2.2.2. Calculation of Transverse Leakage. Transverse leakage is one of the main leakages. The calculation model is shown in Figure 3, where the determination of $\overline{d}$ is complicated. It can be determined by the spiral method on the surface of the rotor [19]:

$$\overline{d_t} = \sqrt{4e^2 + \frac{T^2}{4\pi^2}}, \quad (22)$$

where e is the eccentricity of the screw pump, m, and T is the stator lead, m.

Substituting equation (22) into equation (17), the transverse leakage is

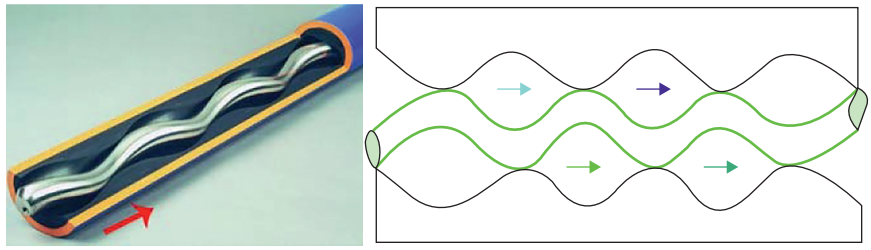

Figure 3: Transverse leakage of all-metal screw pump.

$$q_1 = h\sqrt{4\pi^2 e^2 + \frac{T^2}{4}} \cdot \sqrt{\frac{70\Delta p}{131\rho}}. \tag{23}$$

Equation (23) is the calculation formula for transverse leakage of all-metal screw pumps.

2.2.3. Calculation of Longitudinal Leakage. Longitudinal leakage is one of the main leakages, and its calculation model is shown in Figure 4. There is a relationship:

$$\overline{d}_l = \frac{D_r + D_s}{2}, \tag{24}$$

where D_r is the rotor diameter, m, and D_s is the stator diameter, m.

Combined with formula (17), the longitudinal leakage can be obtained as

$$q_2 = \pi h\left(D_r + D_s\right)\sqrt{\frac{35\Delta p}{262\rho}}. \tag{25}$$

2.2.4. Calculation of Oblique Leakage. The oblique leakage should overcome not only the resistance of the transverse leakage but also the resistance of the longitudinal leakage. Therefore, the amount of the oblique leakage is relatively small, which is the secondary leakage of the screw pump.

It can be known from the screw pump leakage mechanism that the oblique leakage, the transverse leakage, and longitudinal leakage have the following relationship:

$$\frac{1}{q_3} = \frac{1}{q_1} + \frac{1}{q_2}. \tag{26}$$

So, we can get

$$q_3 = \frac{q_1 q_2}{q_1 + q_2}. \tag{27}$$

Combining formulas (23), (25), and (27), we can calculate the oblique leakage formula as

$$q_3 = \sqrt{\frac{70\Delta p}{131\rho}} \times \frac{h\sqrt{4\pi^2 e^2 + (T^2/4)}\left(D_r + D_s\right)}{\sqrt{16e^2 + (T^2/\pi^2)} + D_r + D_s}. \tag{28}$$

Combining transverse leakage, longitudinal leakage, and oblique leakage, the total leakage is

$$q = h\sqrt{\frac{70\Delta p}{131\rho}} \cdot \left[\sqrt{4\pi^2 e^2 + (T^2/4)} + \frac{\pi\left(D_r + D_s\right)}{2} + \frac{\sqrt{4\pi^2 e^2 + (T^2/4)}\left(D_r + D_s\right)}{\sqrt{16e^2 + (T^2/\pi^2)} + D_r + D_s}\right]. \tag{29}$$

Equation (29) is the formula for calculating the total leakage of the all-metal screw pump.

3. Performance Experiments

In order to verify the accuracy of the leakage model, laboratory experiments were conducted by using a special experimental platform, as shown in Figure 5. The experimental system includes the control system, fluid system, and data collection system. The control system is composed of a computer and a console, which is responsible for sending instructions to the fluid system; the fluid system is composed of a screw pump and a motor, which is responsible for the fluid transmission; the data collection system is composed of a flow meter and a pressure gauge, which is responsible for collecting data during the experiment. The systems are tightly coordinated and safe.

The experiment uses a single-head screw pump, as shown in Figure 6. First, the control system transmits instructions to the motor, and then the motor drives the screw pump to rotate. In order to conveniently record the input torque of the screw pump, a torque meter is installed between the motor and the screw pump. After measurement, such as pressure gauge and flow meter, it finally flows into the liquid pool. The whole system is a circulation system.

The experiment was performed under safe and reliable conditions. By adjusting the valve, the pressure difference between the inlet and outlet was changed. The experimental fluid was hydraulic oil, viscosity was 60 mPa·s, and the ambient temperature was 20°C. The experimental pumps were two commercial pumps with different clearances, and the calculation formula of the gap between the stator and the rotor is shown in formula (30). The specific models are shown in Table 1.

$$\delta = \frac{D_s - D_r}{2}, \tag{30}$$

where δ is the gap value, m.

4. Results and Discussion

4.1. Model Validation. According to the model, the theoretical leakage amount can be calculated, and the actual

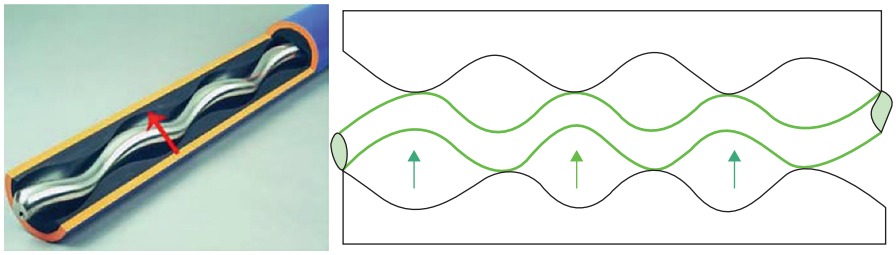

Figure 4: Longitudinal leakage of all-metal screw pump.

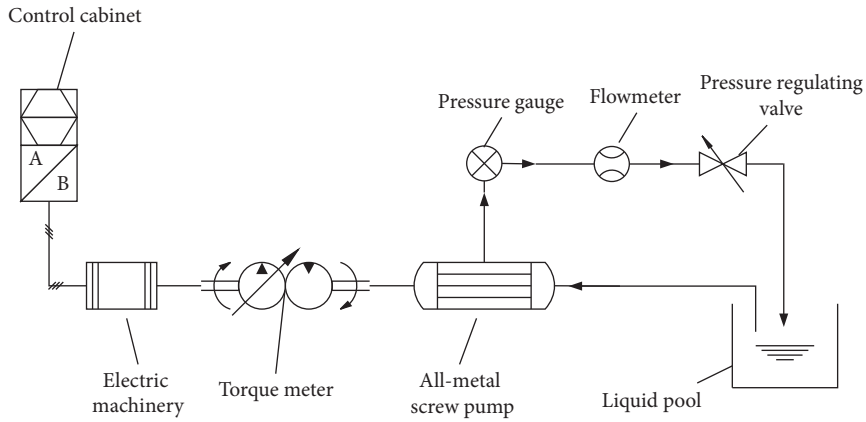

Figure 5: All-metal screw pump performance experiment flowchart.

(a) (b)

Figure 6: Physical picture of all-metal screw pump for experiment. (a) The actual device in the experiment. (b) Screw pump rotor physical map.

Table 1: Geometric dimensions of experimental all-metal screw pump.

Pump type	q_r (ml/r)	T (mm)	e, (mm)	d_r (mm)	δ (mm)
JDGLB160	160	160	5	50	0.1
JDGLB320	320	220	7	56	0.15

leakage amount can be calculated according to the experimental results, and the two are compared and analyzed, as shown in Figure 7. The calculation method of the leakage amount in the experiment can be calculated by the following formula:

$$q = \frac{1440nq_r \times 10^{-6} - Q}{86400}, \tag{31}$$

where Q is the actual displacement of the pump, m^3/d, and q_r is the theoretical displacement of a single revolution, ml/r.

Figures 7(a) and 7(b), respectively, show the experimental results of two different types of pumps. It can be seen from the figure that no matter what type of pump, as the pressure difference increases, the amount of leakage gradually increases, but the increasing trend is gradually decreasing. It is worth noting that compared to the JDGLB160 screw pump with a smaller clearance value, the leakage of the screw pump of the model JDGLB350 is greater.

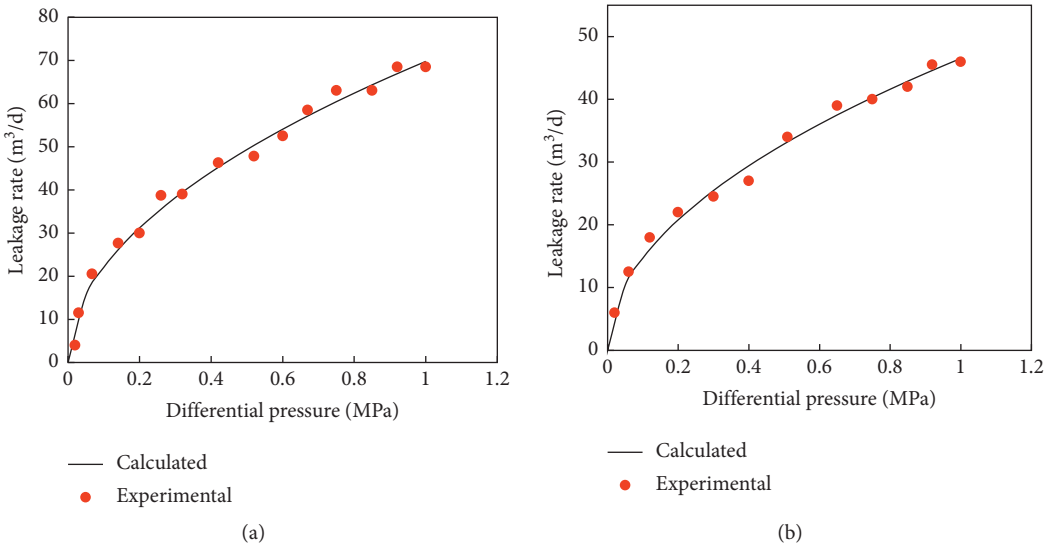

Figure 7: Comparison between model results and experimental results. (a) Results for JDGLB320. (b) Results for JDGLB160.

It can be seen from Figure 7 that the experimental results agree well with the model results. The comparison of the relative error results is shown in Figure 8. The overall error is less than 5%. The results show that the accuracy of the model is well verified.

It is worth noting that the experimental results also show that although increasing the rotational speed is beneficial to increasing the output of the pump, it has no obvious effect on reducing the amount of leakage, which is consistent with the model results.

4.2. Influencing Factor Analysis and Model Verification with Variable Parameters. By further analyzing the derived model, it can be seen from equation (29) that the pump leakage is not only related to the pressure difference but also related to the fluid density and the parameters of the pump itself.

At the same time, in order to verify whether the calculation results of the model are consistent with the theoretical results when other parameters are changed, we change fluid density values and change the gap values of the pump to continue the experiments. We also compare the experimental results with the theoretical calculation results (Figures 9 and 10).

4.2.1. Gap Height. The height of the gap between the stator and rotor of the all-metal screw pump is a very important structural parameter of the pump. In order to analyze the effect of the gap height on the amount of leakage, a sensitivity analysis is performed on the gap height h, and the theoretical calculation results are compared with the experimental results, as shown in Figure 9.

It can be seen from Figure 9 that the experimental results are in good agreement with the theoretical calculations even after changing the h values, which further verifies the accuracy of the model. It can also be seen that as the pressure difference increases, the amount of leakage gradually

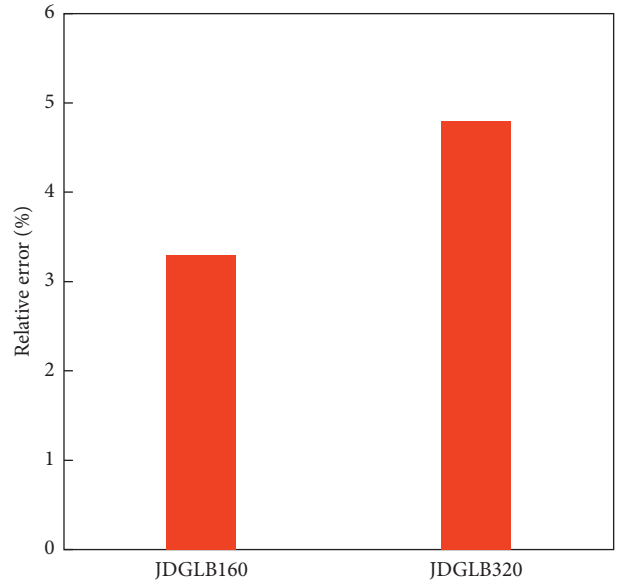

Figure 8: Relative error of comparison results.

increases, but the rate of growth is declining; at the same time, it can be seen that different gap values have a great impact on the amount of leakage, that is, at the same pressure, the larger the gap value, the greater the amount of leakage, and this disparity is more obvious in the case of high pressure difference.

4.2.2. Fluid Density. In order to investigate the effect of fluid density on the amount of leakage and verify the accuracy of the model when changing the fluid density values, the experiments of changing the fluid density values were carried out, as shown in Figure 10.

It can be seen from Figure 10 that the experimental data are in good agreement with the model calculation results,

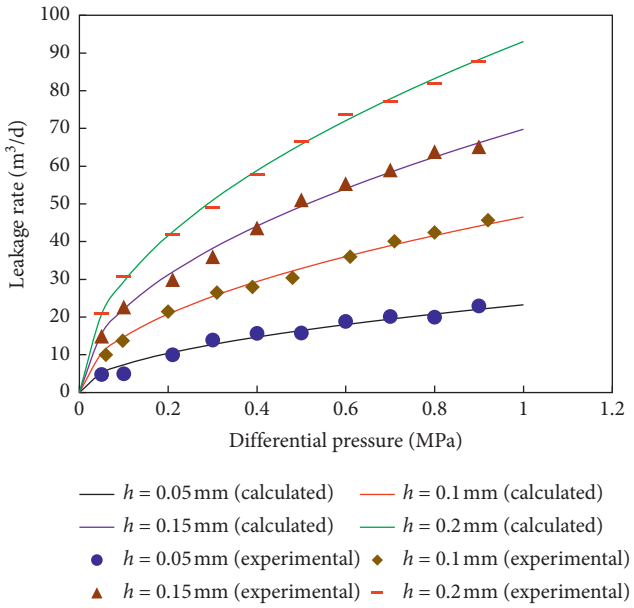

Figure 9: The effect of gap height on leakage.

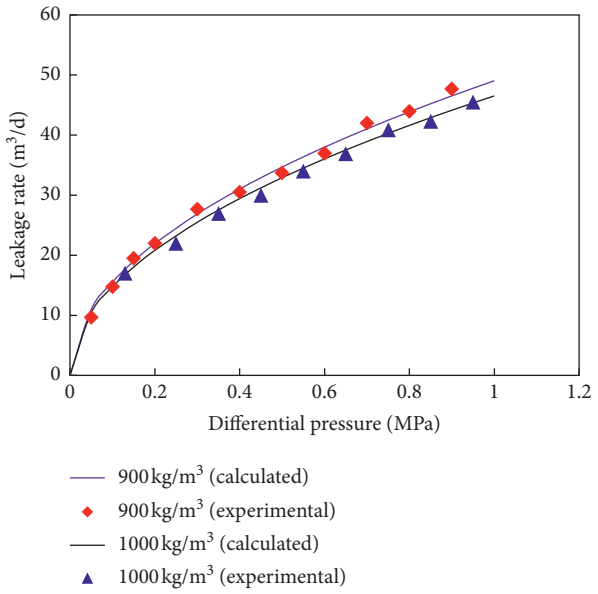

Figure 10: The effect of density on leakage.

under the condition of varying fluid density values, which further verifies the accuracy of the model.

It can also be seen that under certain other conditions, the amount of leakage decreases with increasing density, but compared to the structure parameters of the pump itself, the density of the fluid has a smaller effect on the amount of leakage, which is a secondary influencing factor.

5. Conclusions

In this paper, a new all-metal screw pump leakage model is established with full consideration of inertial forces, which will help to better understand the performance of all-metal screw pumps. The following conclusions are drawn:

(1) Based on the concentric annular gap flow theory, ignoring the viscous pressure drop, and research on three aspects of transverse leakage, longitudinal leakage, and oblique leakage, a new metal screw pump leakage model was established.

(2) The model results agree well with the experimental results, which verifies the accuracy of the model. At the same time, the model can also guide the optimization of the structural parameters of the pump.

(3) We change other parameters to continue the experiment and compare the experimental results with the theoretical calculation results. The results show that the model calculation results agree well with the experimental results, which further proves the accuracy of the model.

(4) According to the sensitivity analysis of the parameters, it can be known that the gap height is the main factor affecting the pump leakage, and the fluid density has an effect on the leakage but is a secondary factor.

Nomenclature

Δp_0: Single-stage pressure difference between the pumps, Pa
Δp_1: Inertia pressure loss at the inlet section, Pa
Δp_2: Inertia pressure loss at the outlet section, Pa
R_0: Outer radius of the concentric ring, m
r_0: Inner radius of the concentric ring, m
h: Clearance height, m
u: Fluid velocity, m/s
E: Fluid kinetic energy, J
N: Inertial power at entrance, W
$\overline{d}$: The average diameter of the gap, m
μ: Fluid viscosity, Pa·s
L: Gap length, m
Δp: Total pressure loss, Pa
q_1: Transverse leakage, m^3/s
q_2: Longitudinal leakage, m^3/s
q_3: Oblique leakage, m^3/s
q: Total leakage, m^3/s
D_r: Rotor diameter, m
D_s: Stator diameter, m
Q: Theoretical flow rate, m^3/d
q_r: Theoretical displacement of a single revolution, ml/r.

Data Availability

The data used to support the findings of this study are available from the corresponding author upon request.

Conflicts of Interest

The authors declare that they have no conflicts of interest.

Acknowledgments

This research was supported by the "National Science and Technology Major Project Program" (2017ZX05009-003, 2017ZX05072006-002, and 2017ZX05032-004-006).

References

[1] M. Lehman, "Progressing cavity pumps in oil and gas production," *World Pumps*, vol. 2004, no. 457, pp. 20–22, 2004.

[2] M. Lehman, "Large progressing cavity pumps for oil field transfer application," *World Pumps*, vol. 2005, no. 467, pp. 28–30, 2005.

[3] L. Dunn, C. Matthews, and T. Zahacy, "Progressing cavity pumping system Applications in heavy oil production," in *Proceedings of the SPE International Heavy Oil Symposium*, Calgary, Canada, June 1995.

[4] L. Ocanto and A. Rojas, "Progressing cavity pump pattern recognition in heavy and extra-heavy oil cold production," in *Proceedings of the SPE International Thermal Operations and Heavy Oil Symposium*, Porlamar, Venezuela, March 2001.

[5] M. A. Ramos, J. C. Brown, M. D. C. Rojas, O. Kuyuco, and J. G. Flores, "Producing extra-heavy oil from the orinoco belt, Cerro Negro area, Venezuela, using bottom-drive progressive cavity pumps," *SPE Production & Operations*, vol. 22, no. 2, pp. 151–155, 2007.

[6] H. Wang, S. Wang, and X. Lv, "The effects of temperature on themechanical and tribological properties of progressing cavity pump NBR stator rubber," *Mechanika*, vol. 22, no. 4, pp. 308–312, 2016.

[7] M. Li, D. Jiang, H. Guo et al., "Study on clearance optimization of all-metal screw pumps: experiment and simulation," *Mechanika*, vol. 23, no. 5, pp. 735–742, 2017.

[8] S. G. Noonan, W. Klaczek, K. D. Piers, L. L. Seince, and S. Jahn, "Quest to validate and define performance for the high volume metallic stator PCP at 250C," in *Proceedings of the International Thermal Operations and Heavy Oil Symposium*, Calgary, Canada, October 2008.

[9] K. Bybee, "First metal-PCP SAGD field test shows promise for heavy-oil hot production," *Journal of Petroleum Technology*, vol. 60, no. 7, pp. 70–73, 2015.

[10] K. Bybee, "Experience with metal PCPs in a Cuban heavy-oil field," *Journal of Petroleum Technology*, vol. 61, no. 7, pp. 51–53, 2015.

[11] R. Arystanbay, W. Bae, H. X. Nguyen, S. Ryou, W. Lee, and T. Jang, "Succesful application of metal PCP rechnology to maximize oil recovery in SAGD process," in *Proceedings of the SPE Heavy Oil Conference and Exhibition*, Kuwait City, Kuwait, December 2011.

[12] M. Arredondo, D. Caballero, R. Morety, A. Delgado, and B. Ortegano, "All metal PCP experiences in orinoco belt," in *Proceedings of the SPE Artificial Lift Conference & Exhibition-North America*, Houston, TX, USA, October 2014.

[13] E. E. Paladino, J. A. Lima, R. Almeida, and B. W. Assmann, "Computational modeling of the three-dimensional flow in a metallic stator progressing cavity pump," in *Proceedings of the SPE Progressing Cavity Pumps Conference*, Houston, TX, USA, April 2008.

[14] E. E. Paladino, J. A. Lima, P. A. S. Pessoa, and R. F. C. Almeida, "Computational 3D simulation of the flow within progressing cavity pumps," in *Proceedings of the 20th International Congress of Mechanical Engineering-COBEM*, Gramado, Brazil, November 2009.

[15] E. E. Paladino, J. A. Lima, P. A. S. Pessoa, and R. F. C. Almeida, "A computational model for the flow within rigid stator progressing cavity pumps," *Journal of Petroleum Science and Engineering*, vol. 78, no. 1, pp. 178–192, 2011.

[16] S. F. Andrade, J. V. Valério, and M. Carvalho, "Asymptotic model of the 3D flow in a progressing-cavity pump," *SPE Journal*, vol. 16, no. 2, pp. 451–462, 2011.

[17] J. Chen, H. Liu, F. Wang, G. Shi, G. Cao, and H. Wu, "Numerical prediction on volumetric efficiency of progressive cavity pump with fluid-solid interaction model," *Journal of Petroleum Science and Engineering*, vol. 109, pp. 12–17, 2013.

[18] V. W. F. de Azevedo, J. A. de Lima, and E. E. Paladino, "A 3D transient model for the multiphase flow in a progressing-cavity pump," *SPE Journal*, vol. 21, no. 4, pp. 1458–1469, 2016.

[19] J. Gamboa, A. Olivet, J. Iglesias, and P. Gonzalez, "Understanding the performance of a progressive cavity pump with a metallic stator," in *Proceedings of the 23rd International Pump User Symposium*, Los Teques, Venezuela, March 2002.

[20] J. Gamboa, A. Olivet, and S. Espin, "New approach for modeling progressive cavity pumps performance," *Journal of Petroleum Technology*, vol. 56, no. 5, pp. 51–53, 2003.

[21] P. A. S. Pessoa, E. E. Paladino, and J. A. Lima, "A simplified model for the flow in a progressive cavity pump," in *Proceedings of the 20th International Congress of Mechanical Engineering-COBEM*, Gramado, Brazil, November 2009.

[22] T. Nguyen, H. Tu, E. Al-Safran, and A. Saasen, "Simulation of single-phase liquid flow in progressing cavity pump," *Journal of Petroleum Science and Engineering*, vol. 147, pp. 617–623, 2016.

[23] K. Gui, J. Wang, and Q. Wang, *Engineering Fluid Dynamics*, Science Press, Beijing, China, pp. 105–109, 2015.